Gondwana Research 41 (2017) 222–234

Contents lists available at ScienceDirect

Gondwana Research

journal homepage: www.elsevier.com/locate/gr

Sandstone provenance and tectonic evolution of the Xiukang Mélange from Neotethyan subduction to India–Asia collision (Yarlung-Zangbo suture, south Tibet)

Wei An [a], Xiumian Hu [a,*], Eduardo Garzanti [b]

[a] State Key Laboratory of Mineral Deposits Research, School of Earth Sciences and Engineering, Nanjing University, Nanjing 210023, China
[b] Department of Earth and Environmental Sciences, Università di Milano-Bicocca, Milano 20126, Italy

ARTICLE INFO

Article history:
Received 10 January 2015
Received in revised form 2 August 2015
Accepted 14 August 2015
Available online 21 September 2015

Keywords:
Xiukang Mélange
Provenance analysis
Sandstone blocks
Yarlung-Zangbo suture zone
India–Asia collision
Himalayan orogen

ABSTRACT

The Xiukang Mélange of the Yarlung-Zangbo suture zone in south Tibet documents low efficiency of accretion along the southern active margin of Asia during Cretaceous Neotethyan subduction, followed by final development during the early Paleogene stages of the India–Asia collision. Here we present integrated petrologic, U–Pb detrital-zircon geochronology and Hf isotope data on different types of sandstone blocks in the Xiukang Mélange. Three groups of sandstone blocks with different provenance and depositional setting are distinguished by their petrographic, geochronological and isotopic fingerprints. Blocks of turbiditic quartzarenite originally sourced from the Indian continent were deposited in pre-Cretaceous time on the northernmost edge of the Indian passive margin and eventually involved into the mélange at the early stage of the India–Asia collision. Two distinct groups of volcaniclastic-sandstone blocks were derived from the central Lhasa block and Gangdese magmatic arc. One group was deposited in the trench and/or on the trench slope of the Asian margin during the early Late Cretaceous, and the other group in a syn-collisional basin just after the onset of the India–Asia collision in the Early Eocene. The largely erosional character of the Asian active margin in the Late Cretaceous is indicated by the scarcity of off-scraped trench-fill deposits and the relatively small subduction complex developed during limited episodes of accretion. The Xiukang Mélange was finally structured in the Late Paleocene/Eocene, when sandstone blocks of both Indian and Asian origin were progressively incorporated tectonically in the suture zone of the nascent Himalayan Orogen.

1. Introduction

Studying the suture zone of an orogenic belt such as the Himalayas is fundamental to reconstruct the style of tectonic growth during the early stage of continent–continent collision. Different types of sedimentary successions, deposited prior to collision along the distal edge of active and passive continental margins or in the intervening oceanic basin, can be involved in the formation of a mélange within the suture zone. These include turbidites accumulated in the trench and/or on the trench slope of the active margin (Okada, 1989; Underwood and Moore, 1995), as well as on the continental rise of the passive margin along the opposite side of the subducting ocean. The former are generally derived transversally from the arc, and consequently reflect its magmatic and erosional history, whereas the latter are fed from a continental block and thus display a markedly different mineralogical and geochronological signature. In active margins characterized by tectonic erosion, the fate of trench deposits, oceanic sediments and seamounts is to be largely subducted through the subduction channel (von Huene and Scholl, 1991; Clift and Vannucchi, 2004). During episodes of accretion, however, they may be partly off-scraped and incorporated into a growing subduction complex and finally deformed during the early collisional stage when the embryonic orogen evolves to a fully developed fold–thrust belt.

Northward subduction of the Neotethyan Ocean during the Cretaceous produced an arc-trench system including the Gangdese arc, the Xigaze forearc basin floored by the Yarlung-Zangbo ophiolite, and a small subduction complex and subduction channel presently documented as part of the mélange zone (Fig. 1). Most previous studies focused on the forearc region, with more limited attention given to the mélange zone (Aitchison et al., 2000; Ziabrev et al., 2004; Cai et al., 2012).

In pioneering studies of the 1980s, the mélange zone was considered as a normal sedimentary succession and termed as Xiukang Group (XBGMR, 1979; Yin and Sun, 1988), or described as a wildflysch with exotic blocks and interpreted as a sedimentary mélange (Tapponnier et al., 1981), or interpreted as tectonic in origin and termed as Yamdrock Mélange (Searle et al., 1987). More recently, it was subdivided into the Dazhuqu and Bainang terranes, interpreted to represent the subduction complex of an intra-oceanic island arc fed by Tethyan oceanic rocks during the Cretaceous (Aitchison et al., 2000; Ziabrev et al., 2004; Aitchison et al., 2007). The type section is exposed around the Xiukang–

* Corresponding author. Tel.: +86 2589683002.
E-mail address: huxm@nju.edu.cn (X. Hu).

http://dx.doi.org/10.1016/j.gr.2015.08.010
1342-937X/

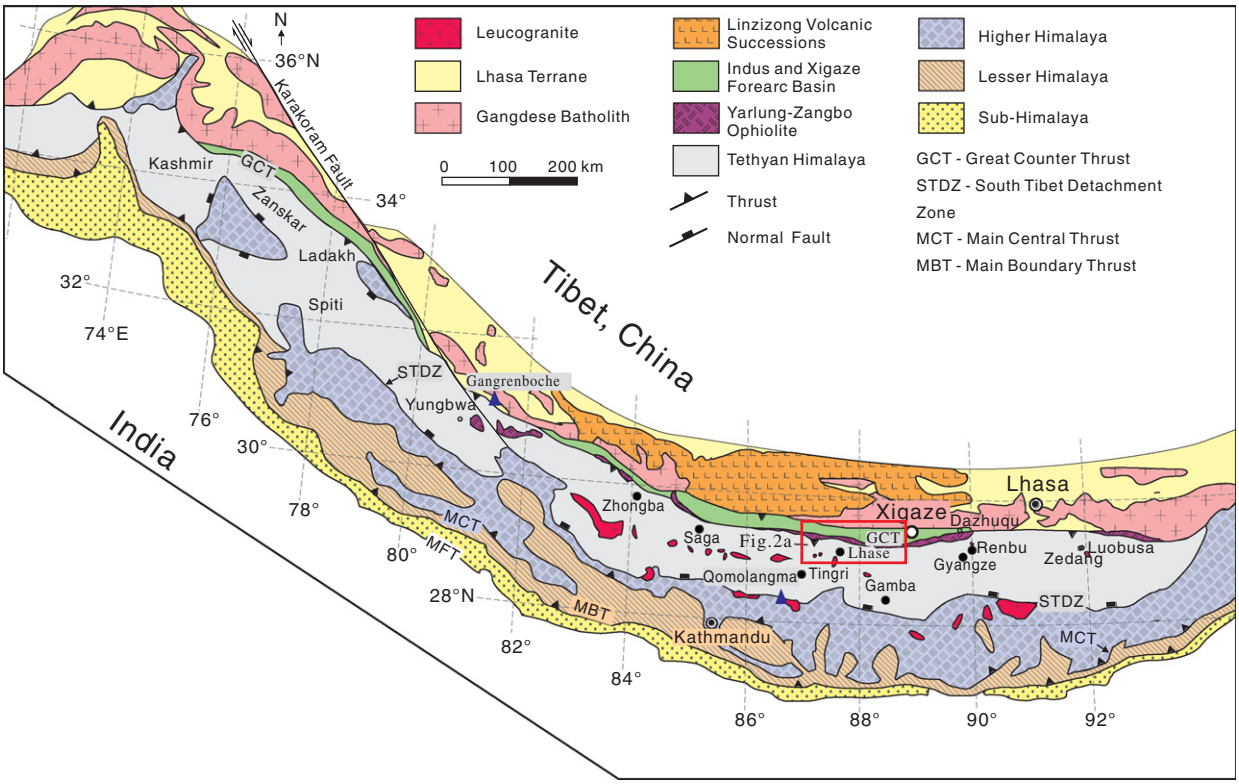

Fig. 1. Simplified geological map of the Himalaya (modified after Pan et al. (2004)). The study area, expanded in Fig. 2, is outlined.

Qianggong villages near the Colha pass (Searle et al., 1987; Yin and Sun, 1988) (Fig. 1), which justifies the term Xiukang Mélange adopted here.

Sandstone blocks were dated by detrital-zircon U–Pb geochronology as Late Cretaceous (~71 Ma) and interpreted to have been accreted before deposition of the overlying, uppermost Cretaceous Rongmawa Formation which records transition from lower abyssal plain to upper trench sedimentation (Cai et al., 2012). The subsequent syn-collisional evolution of the Xiukang Mélange was scarcely considered, although syn-collisional sediments interpreted to be foreland-basin deposits have been reported in the Renbu area, ~170 km east of our study area (G.W. Li et al., 2015). The provenance of blocks contained in the mélange is also debated. Some geologists concluded that the Xiukang Mélange contains mostly sediments with Indian affinity and seamounts of Neotethyan crust (Ziabrev, 2002; Shen et al., 2003a,b; Dupuis et al., 2006), whereas others considered that the sandstone blocks were principally derived from the Lhasa block in the north (Cai et al., 2012).

The aim of the present article is to unravel the early geological evolution of the India–Asia continental collision from a suture-zone perspective. We present new detailed petrological, detrital zircon U–Pb geochronology and Hf isotope data on different types of sandstone blocks contained in the Xiukang Mélange of the Yarlung-Zangbo suture zone in south Tibet (Fig. 2), and on northern Tethyan Himalaya quartzarenites of the Upper Jurassic–Lower Cretaceous Weimei Formation, found in fault contact with the Xiukang Mélange and studied here for comparison. The results allowed us to determine the provenance and depositional age of three different groups of blocks, and to demonstrate that, unlike other well studied accretionary prisms (e.g. Nankai Trough, Clift et al., 2013; Franciscan complex, Snow et al., 2010; Chugach accretionary complex, Amato et al., 2013), the Xiukang Mélange did not only experience evolution during Cretaceous Neotethyan subduction but chiefly recorded collision between the Asian active margin and the Indian passive margin in the early Paleogene. The importance of the collisional event has never been recognized in the mélange so far.

2. Geological setting

2.1. The Asian active margin

The Lhasa block is a W-E trending tectonic domain that can be subdivided into northern, central, and southern terranes characterized by different magmatic and sedimentary units (Zhu et al., 2011a). In the northern Lhasa block, sedimentary successions are mainly Jurassic and Cretaceous in age but Triassic strata also occur. In the central Lhasa block, Permo-Carboniferous metasedimentary and Upper Jurassic–Lower Cretaceous volcano-sedimentary strata are widespread (Pan et al., 2004; Zhu et al., 2011a and references therein), together with Lower Cretaceous volcanic rocks (e.g., Zenong Group, Zhu et al., 2011a) and Mesozoic plutonic rocks dated between 215 and 95 Ma (Pan et al., 2004; Zhu et al., 2011a and references therein). In the southern Lhasa block, the sedimentary cover is limited and mainly of Late Triassic–Cretaceous age (Pan et al., 2006; Zhu et al., 2008, 2013); magmatic rocks include the Upper Triassic to Paleogene Gangdese arc (Schärer et al., 1984; Wen et al., 2008; Ji et al., 2009) and the Cretaceous to Tertiary non-marine Linzizong volcanic succession (Mo et al., 2008 and references therein). Magmatic rocks emplaced from the Late Triassic to the Eocene (220–40 Ma) display distinct zircon U–Pb-age and Hf-isotope signatures: zircons with negative εHf(t) characterize the central Lhasa block, indicating presence of an ancient crust (Chu et al., 2006; Zhu et al., 2011a); zircons with positive εHf(t) characterize the southern Lhasa block (Chu et al., 2006; Zhang et al., 2007; Ji et al., 2009), suggesting a juvenile crust.

The Xigaze forearc-basin succession, exposed from Renbu in the east to Zhongba in the west over a length of ~500 km and with a maximum width of ~22 km, is traditionally subdivided into the Chongdui, Sangzugang, Ngamring, and Padana Formations, from base to top (Wang et al., 2012). The overlying Paleogene Cuojiangding Group, exposed locally in the Zhongba County, represents the youngest stratigraphic unit documenting syn-collisional fan-deltas deposited on top

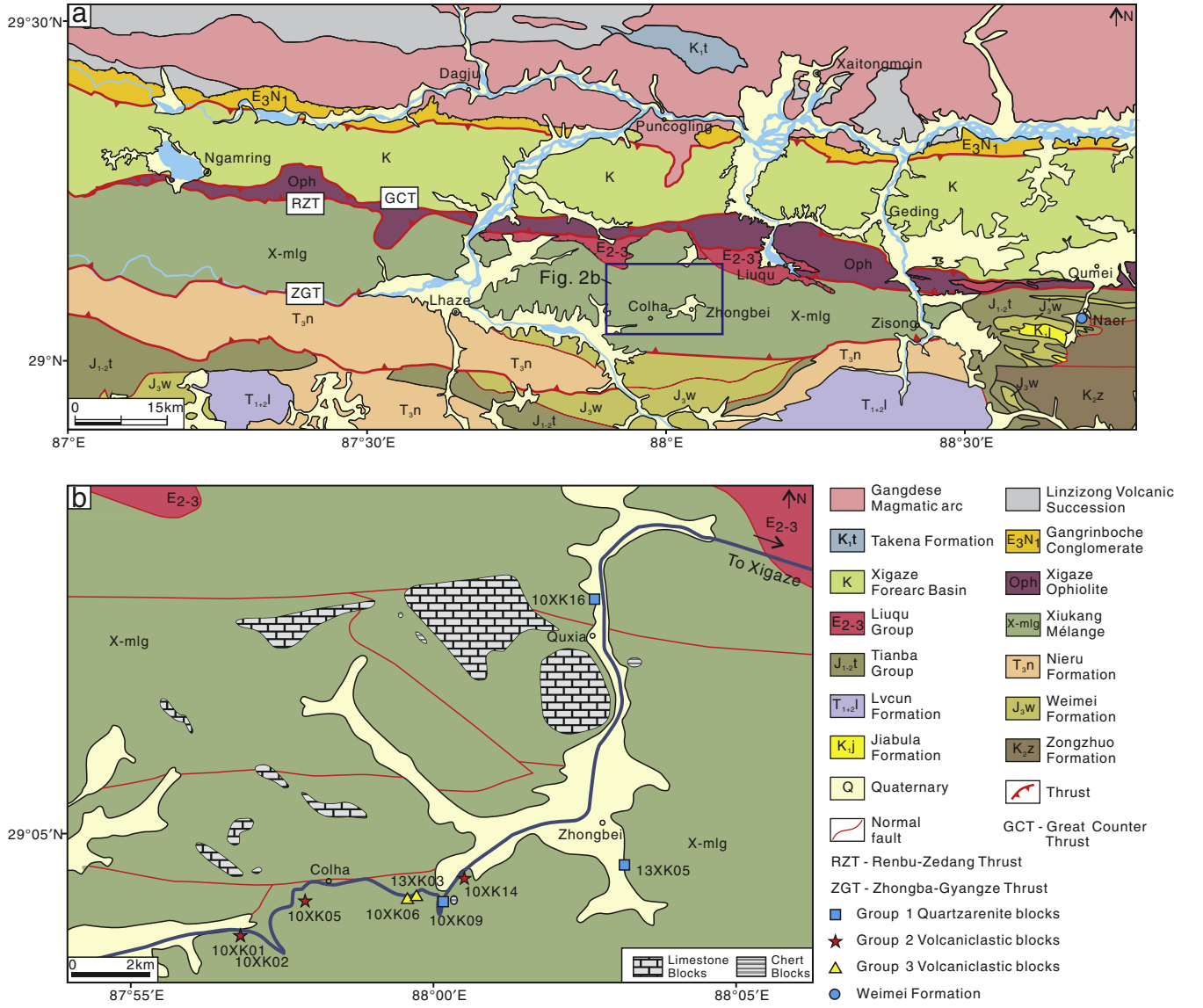

Fig. 2. (a) Geological sketch map of the studied region with circle representing sampling location for the Weimei Formation. Expanded in (b) is the Zhongbei area; squares, stars and triangles represent locations for dated samples of Group 1, Group 2 and Group 3 sandstone blocks, respectively.

of the nascent Himalayan orogenic belt (Ding et al., 2005; Orme et al., 2014; Hu et al., 2016). Sandstone lithofacies and provenance studies (Einsele et al., 1994; Dürr, 1996), supplemented by detrital-zircon U–Pb age and Hf isotopic data (Wu et al., 2010; Aitchison et al., 2011; An et al., 2014), indicate that detritus was dominantly derived from the Gangdese arc, with additional contributions from the central Lhasa block and from reworking of the Sangzugang Formation within the basin.

2.2. The Yarlung-Zangbo suture zone and the Xiukang Mèlange

The Yarlung-Zangbo Ophiolite, composed of mantle peridotites, cumulates, gabbros, sheeted dikes, pillow lavas and radiolarian cherts, crops out from Luobusa in the east to Yungbwa in the west. Its central part between Dazhuqu and Sangsang is termed the Xigaze Ophiolite. The age of magmatism, previously assessed at 120 ± 10 Ma (Göpel et al., 1984), has been later refined at 128–123 Ma (Malpas et al., 2003; Dai et al., 2013 and references therein). Formerly interpreted as produced along a slow-spreading mid-ocean ridge (Nicolas et al., 1981; Girardeau et al., 1985a,b), recent studies have favored formation in a supra-subduction setting (Bédard et al., 2009; Hébert et al., 2012) and forearc spreading (Dai et al., 2013).

The Xiukang Mélange, currently 10–20 km-wide and in tectonic contact with the Yarlung-Zangbo Ophiolite along the Renbu-Zedang thrust fault in the north and with Tethyan Himalayan strata along the Zhongba-Gyangze fault in the south, has been traditionally interpreted to be part of an accretionary prism (Tapponnier et al., 1981; Gao and Tang, 1984; Searle et al., 1987; Cai et al., 2012). The Xiukang Mélange, including exotic blocks of sandstone, limestone, chert and basalt with various sizes and ages, displays a typical block-in-matrix fabric. The generally deformed matrix is represented by upper Triassic–lower Aptian abyssal chert, siliceous mudstone and local turbidites showing N-S trending stretching lineation and top-to-south S-C fabrics (Gao and Tang, 1984; Cai et al., 2012). The occurrence of *Globotruncanas* within the limestone blocks suggested a post-Late Cretaceous age for the formation of the mélange (Tapponnier et al., 1981). Analyses of sandstone blocks led to infer contrasting sources: geochemical evidence favored provenance from the Indian continent (Dupuis et al., 2006), whereas petrologic and zircon U–Pb analysis indicated ages not younger than 71 Ma and origin from the Lhasa block (Cai et al., 2012; G.W. Li et al., 2015).

The abundant limestone blocks, varying in size from cm to km (Fig. 3a), are mostly bioclastic, with Middle–Late Permian crinoids and bryozoans (Fig. 4a), and Early Triassic, Early Jurassic and Late Cretaceous foraminifera (Tapponnier et al., 1981; Jin et al., 2015 and references therein). These exotic blocks have been variously interpreted to represent either remnants of seamounts within the Neotethys Ocean (Wang and Mu, 1980), or of a carbonate platform situated on the northern fringe of Gondwana (Guo et al., 1991). Subsequent studies of the brachiopod fauna have documented transitional/mixed characters between Cathaysian and Gondwanan faunas, favoring deposition on the outer peri-Gondwanan shelf or on seamounts within Neotethys (Shen et al., 2003a,b). Blocks from seamounts within the Neotethys Ocean, as indicated by limestones and cherts directly deposited on OIB-type basalt, have been reported recently in Zhongba, 400 km west of our studying area (Dai et al., 2012) (Fig. 1). Decimetric to metric basaltic blocks appear occasionally (Fig. 3b, Fig. 4b). They are mainly porphyritic and/or amygdaloidal, have experienced low-grade hydrothermal metamorphism, and display within-plate-basalt geochemical affinity, similar to Indian-Reunion "hotspot" lavas (Dupuis et al., 2005). Metric blocks of radiolarian chert have been identified as two groups, Middle–Upper Triassic ones with continental-margin affinity indicated by MnO/TiO_2 of ~ 0.36 and Ce/Ce^* of ~1.15 and Upper Jurassic–Lower Cretaceous ones with oceanic-basin affinity and MnO/TiO_2 of ~1.24 and Ce/Ce^* of ~1.03 (Zhu et al., 2005).

2.3. The Indian passive margin

The Tethyan Himalaya is traditionally subdivided into northern and southern domains (Liu and Einsele, 1994; Jadoul et al., 1998), separated by the Gyirong–Kangmar thrust (Ratschbacher et al., 1994). The southern Tethyan Himalaya is characterized by Paleozoic to Eocene shelfal carbonates and terrigenous strata (Willems et al., 1996; Wang et al., 2002), whereas the northern Tethyan Himalaya consists of corresponding outer shelf, continental slope and rise deposits. These include the Weimei Formation (Upper Jurassic/Lower Cretaceous turbiditic quartzarenites), the Rilang Formation (Lower Cretaceous volcaniclastic sandstones with intercalated mudrocks), the Gyabula Formation (mid-Cretaceous shales and siliceous rocks) and the Chuangde Formation (Upper Cretaceous oceanic red beds) (Liu and Einsele, 1994; Hu et al., 2008). The Middle Paleocene to Eocene, largely volcaniclastic sandstones and mudrocks (e.g. Sangdanlin and Zheya Formations in Saga, Enba and Zhaguo Formations in Tingri–Gamba) represent syncollisional deposits south of the Yarlung-Zangbo suture zone (Ding et al., 2005; Wang et al., 2011; Hu et al., 2012; DeCelles et al., 2014; Hu et al., 2015b; J. Li et al., 2015).

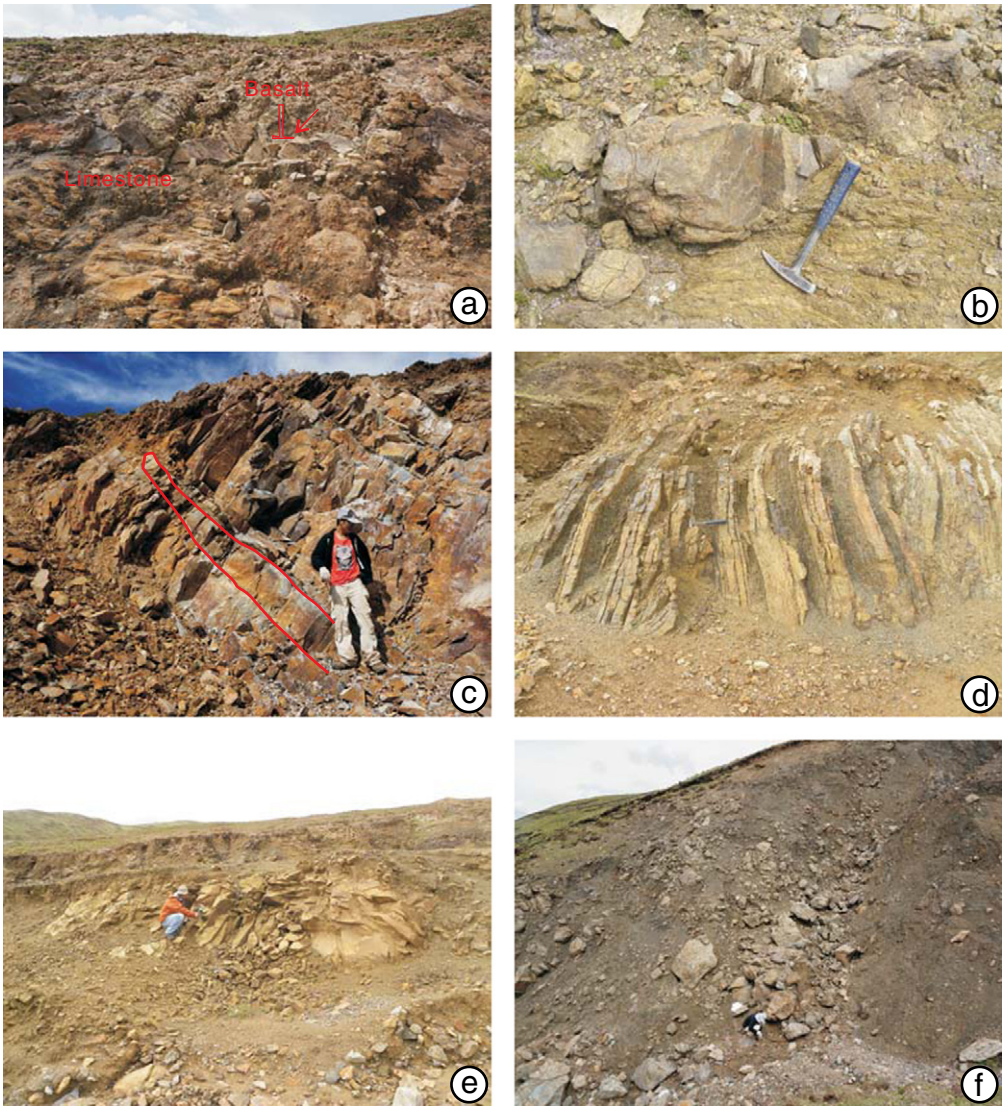

Fig. 3. Outcrops of blocks in the Xiukang Mélange: a) depositional contact between blocks of limestone and basalt, hammer highlighted by arrow indicates scale; b) cm-scale quartzarenite of Group 1; c) m-scale quartzarenite of Group 1; d and e) m-scale volcaniclastic turbidites of Group 2; f) m-scale volcaniclastic sandstones of Group 3.

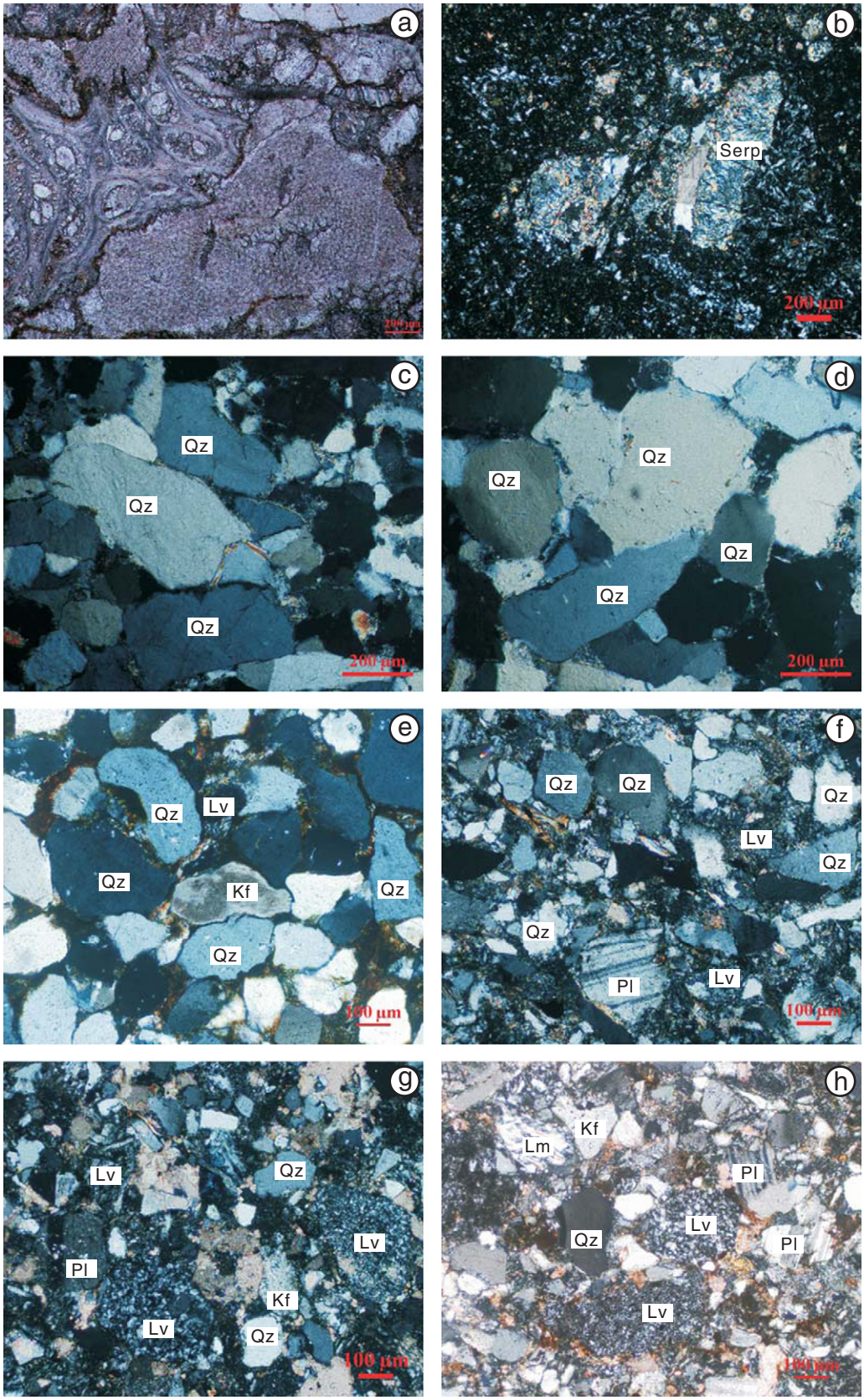

Fig. 4. Microphotographs: (a) bioclastic limestone with crinoids and bryozoans (limestone block, 13ZB-B06); (b) serpentinized peridotite (13XK02); (c) and (d) Weimei quartzarenites (13QM03, 14QM04); (e) Group 1 quartzarenite (10XK10); (f) Group 2 volcaniclastic sandstone (10XK01); (g) and (h) Group 3 volcaniclastic sandstone (10XK06, 13XK04). (Qz = quartz; Kf = K-feldspar; Pl = plagioclase; Lm = metamorphic lithic fragments; Lv = volcanic lithic fragments).

2.4. Onset of the India–Asia collision

The timing of the India–Asia collision has long been disputed (Yin and Harrison, 2000; Garzanti, 2008). Most stratigraphic, provenance and paleomagnetic studies suggest that the initial contact between India and Asia occurred at 55 ± 5 Ma (e.g. Huang et al., 2010; Najman et al., 2010; Lippert et al., 2014; Yang et al., 2015 and references therein). An alternative has been proposed that India collided first with an intra-oceanic arc at ~55 Ma and eventually with Asia at ~35 Ma (Aitchison et al., 2007). However, a syncollisional basin was developed on top of the Xigaze forearc basin, constraining the onset of the India–Asia collision as between 66 and 58 Ma (Hu et al., 2016). Meanwhile, detritus derived from the Lhasa Block in Middle Paleocene to Eocene Tethyan Himalayan successions (Sangdanlin Formation in Saga, Enba Formation in Tingri–Gamba) indicates that no intra-oceanic arc existed within the Neotethys and that the India–Asia collision began not later than ~58 Ma in southern Tibet (Cai et al., 2011; Wang et al., 2011; Hu et al., 2012; Wu et al., 2014; J. Li et al., 2015), as supported by stratigraphic evidence (Zhang et al., 2012; DeCelles et al., 2014; Hu et al., 2015). A similar age was previously established by stratigraphic and provenance criteria in central Nepal (DeCelles et al., 2004; Najman et al., 2005) and northern India (Garzanti et al., 1987).

3. Methods

Sandstone samples from the Weimei Formation (Fig. 4c and d) and Xiukang Mélange (Fig. 4e, f, g and h) were selected for modal analysis and detrital-zircon geochronology. Over 400 points were counted on 14 samples following the Gazzi-Dickinson method, in which crystals larger than 62 μm are counted as single grains even where included in rock fragments (Ingersoll et al., 1984). The full dataset is presented as Supplementary material. Accessory minerals were separated from 10 sandstone samples by elutriation and magnetic separation. Zircon grains were hand-picked, mounted in epoxy resin, and polished. U–Pb dating of detrital zircons was conducted by LA-ICP-MS at the State Key Laboratory of Mineral Deposits Research, Nanjing University, following Jackson et al. (2004). To avoid grain-to-grain bias and treat all samples equally, the laser spot was always placed in the core of the zircon grains. Various beam diameters (18–35 μm) were used, depending on the size of zircon grains. The weighted $^{206}Pb/^{238}U$ age of Mud Tank Zircon obtained is 726.7 ± 5.4 Ma (n = 17), consistent with the predicted value (TIMS age = 732 ± 5 Ma; Black and Gulson, 1978). GLITTER 4.4 was used for calculating results and relevant isotopic rates (Jackson et al., 2004). Age calculations and concordia diagrams were created using Isoplot 4.0 (Ludwig, 2011). The interpretation of zircon ages was based on $^{206}Pb/^{238}U$ ages for grains <1000 Ma and on $^{207}Pb/^{206}Pb$ ages for grains >1000 Ma. Zircon grains older than 200 Ma with discordance <10% and those younger than 200 Ma with discordance <20% were used. Dickinson and Gehrels (2009) concluded that the weighted mean age of two or more grains overlapping in age at 1σ (YC1σ(2+)) is the most robust indicator of maximum depositional age, as tested for strata derived from an active magmatic arc. U–Pb data are summarized in Table 1; the complete dataset and sample locations are provided as Supplementary material.

In-situ zircon Hf isotopic analyses were conducted on spots immediately adjacent to the site used for the U–Pb age analysis. Hf isotopic compositions were determined with a Thermo Scientific Neptune Plus MC-ICP-MS coupled to a New Wave UP193 solid-state laser-ablation system at the State Key Laboratory for Mineral Deposits Research, Nanjing University. Zircon grains were ablated with a beam diameter of 35 μm with an 8-Hz laser repetition rate, or of 25 μm with a 7-Hz laser repetition rate, and with energy >15.5 J/cm^2. The Mud Tank standard was analyzed in every run, yielding $^{176}Hf/^{177}Hf$ = 0.282489 ± 0.000030 (2σ; n = 40), which is identical to the literature value of $^{176}Hf/^{177}Hf$ = 0.282522 ± 0.000042 (2σ; n = 2335) (Griffin et al., 2007). The complete dataset is provided as Supplementary material.

4. Results

Petrographic analysis and detrital-zircon geochronology indicate that the Xiukang Mélange contains three distinct groups of sandstone blocks. Blocks of Group 1, most common and with outcrops up to a few kilometers in size, consist of thick-bedded or lenticular quartzarenite intercalated with thin-bedded gray siliceous mudstone (Fig. 3c). Blocks of Group 2 consist of lithic-rich sandstone rhythmically-interbedded with mudstone in m-size outcrops (Fig. 3d, e). Blocks of Group 3 consist of lithic-rich sandstone without primary structures, exposed sparsely near the Lhasa–Kathmandu main road (Fig. 3f).

Group 1 quartzarenites (average composition QFL = 93:2:5, QmFLt = 91:2:7, Figs. 4e and 5a) consist of mainly angular to subrounded monocrystalline and subordinately polycrystalline quartz (Fig. 4c, d), with a few feldspars (K-feldspar > plagioclase; Fig. 4e), and mainly low-rank metamorphic and volcanic or rarely sedimentary lithic fragments (Fig. 5b). Of the 211 usable ages obtained from three samples (10XK09, 10XK16 and 13XK05), 209 are pre-Ordovician with main peaks at 950 Ma and 514 Ma (Fig. 6). The youngest ages are 224 ± 3 Ma, 441 ± 7 Ma and 486 ± 7 Ma, with discordance of 0%,

Table 1
Summarized characteristics of detrital zircon U–Pb ages of sandstone samples in the Xiukang mélange and Weimei Formation.

Formation	Sample	Analyzed numbers of zircon grain	Percentage of the Mesozoic ages	Maximum depositional Age (Ma)	YDZ[a]	YSG[b]	YPP[c]	YC1σ(2+)[d]	YC2σ(3+)[e]
Group 3	13XK03	n = 69	87% (60 out of 69)	59.3 ± 0.8	54.3 + 1.7/−5.5	55 ± 1	55.3	59.3 ± 0.8 (n = 13)	66.6 ± 0.6 (n = 24)
	10XK06	n = 163	69% (113 out of 163)	54.5 ± 0.6	51.9 + 1.3/−2.2	52 ± 1	56.8	54.5 ± 0.6 (n = 13)	55.9 ± 0.4 (n = 24)
Group 2	10XK14	n = 72	65% (47 out of 72)	98.2 ± 1.0	94.5 + 2.1/−4.2	95 ± 2	98.0	98.2 ± 1.0 (n = 13)	101.2 ± 0.8 (n = 3)
	10XK05	n = 69	23% (16 out of 69)	94 ± 1.4	92.8 + 2.1/−2	93 ± 1	93.6	94 ± 1.4 (n = 2)	95 ± 1.3 (n = 4)
	10XK02	n = 69	12% (8 out of 69)	126.7 ± 3.1	113.0 + 4.5/−4.4	113 ± 2	112.6	126.7 ± 3.1 (n = 3)	129.7 ± 2.7 (n = 4)
	10XK01	n = 62	31% (19 out of 62)	131.8 ± 16	100.8 + 4.7/−4.3	101 ± 2	100.5	131.8 ± 16 (n = 7)	132.7 ± 1.4 (n = 10)
Group 1	13XK05	n = 66	0% (0 out of 66)	518.7 ± 4.5	500.8 + 8.9/−17	502 ± 8	518.4	518.7 ± 4.5 (n = 13)	536.8 ± 3.4 (n = 24)
	10XK16	n = 82	0% (0 out of 82)	514.9 ± 4.1	485.8 + 11/−15	486 ± 7	500.0	514.9 ± 4.1 (n = 13)	539.3 ± 3.3 (n = 20)
	10XK09	n = 63	2% (1 out of 63)	507.9 ± 4.2	223.7 + 7/−6.4	224 ± 3	224.0	507.9 ± 4.2 (n = 12)	507.9 ± 4.2 (n = 12)
The Weimei Formation	13QM03	n = 71	1% (1 out of 71)	528.0 ± 5	229.4 + 8.6/−9.5	229 ± 4	229	528.0 ± 5 (n = 13)	557.8 ± 3.7 (n = 24)

Notes:
[a] YDZ = Age calculated by the "Youngest Detrital Zircon" routine of Isoplot (Ludwig, 2011);
[b] YSG = Youngest single detrital zircon age with 1δ uncertainty;
[c] YPP = Youngest graphical detrital zircon age peak on an age-probability plot or age-distribution curve;
[d] YC1σ(2+) = Weighted mean age (±1σ incorporating both internal analytical error and external systematic error) of youngest cluster of two or more grain ages overlapping in age at 1σ;
[e] YC2σ(3+) = Weighted mean age (±1σ incorporating both internal analytical error and external systematic error) of youngest cluster of three or more grain ages overlapping in age at 2σ (Dickinson and Gehrels, 2009).

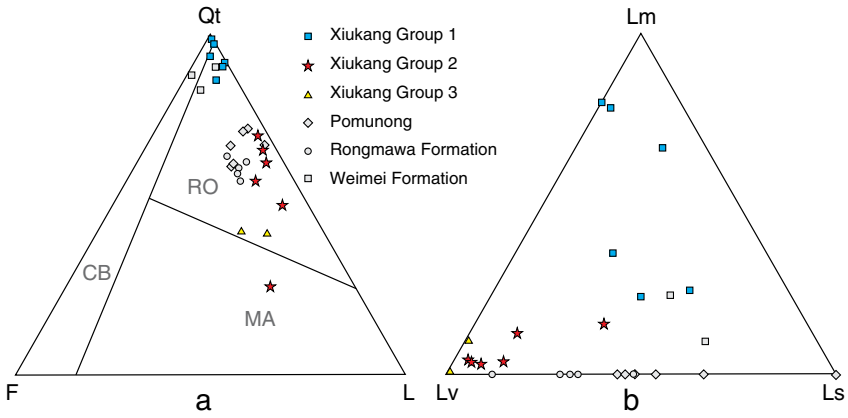

Fig. 5. Sandstone petrography of blocks in the Xiukang Mélange and the Weimei Formation. a) QtFL diagram. Qt = quartz + chert; F = feldspars; L = Lithic fragments. Recycled orogen (RO), magmatic arc (MA), basement uplift (BU), transitional continental (TC) and craton interior (CI) provenance fields after Dickinson (1985); b) LmLvLs diagram. Lm = metamorphic lithic fragments; Lv = volcanic lithic fragments; Ls = sedimentary lithic fragments. Data for the Pomunong Mélange and the Rongmawa Formation are from Cai et al. (2012), for the Weimei Formation from Cai et al. (2011) and Du et al. (2015).

0.2% and 0.6%, respectively. The YC1σ(2+) ages in the three samples are 518 ± 5, 515 ± 4 Ma and 508 ± 4 Ma, respectively.

Group 2 turbidites are litho-quartzose volcaniclastic (average composition QFL = 55:8:37, QmFLt = 53:8:39) with monocrystalline and subordinately polycrystalline quartz grains, feldspars (K-feldspar ≈ plagioclase), and mostly microlitic to felsitic volcanic, common sedimentary (siltstone, shale) and minor low-rank metamorphic lithic fragments (Figs. 4f and 5b). Of the 273 concordant ages obtained from four samples (10XK01, 10XK02, 10XK05 and 10XK14), 90 are Mesozoic (64 of which are between 145 and 93 Ma) (Fig. 7) and 183 are older than 250 Ma. The youngest ages are 93 ± 1 Ma, 95 ± 1 Ma and 95 ± 2 Ma, with discordance of 0%, 0% and 1.1%, respectively. The age pattern is complex, with a main peak at 99 Ma, a smaller one at 133 Ma and numerous small clusters. The YC1σ(2+) ages in the three samples are 132 ± 16, 127 ± 3 Ma and 94 ± 1 Ma, respectively; 69 Mesozoic zircon grains show either positive or negative εHf(t) (from −22.5 to +16.9).

Group 3 sandstones are feldspatho-litho-quartzose volcaniclastic (average composition QFL = 42:18:40, QmFLt = 41:18:41) with dominantly monocrystalline, subangular to rounded quartz grains, common feldspars (plagioclase > K-feldspar), and mostly microlitic to felsitic volcanic and minor sedimentary and low-rank metamorphic lithic fragments (Fig. 4g, h). Zircon, epidote, muscovite and biotite are common accessory minerals in all three groups of sandstone blocks. Among the 232 valid ages obtained from two sandstone blocks (10XK06 and 13XK03), 43 are Paleogene, 106 Cretaceous, 24 Jurassic or Triassic, and 59 pre-Mesozoic and as old as 2649 Ma (Fig. 7). The youngest ages are 52 ± 1 Ma, 53 ± 1 Ma and 54 ± 1 Ma, with discordance of 8%, 6% and −2%. The complex age pattern includes peaks at 56, 67, 88, 98, 115, 125 Ma, and numerous other smaller age clusters. The YC1σ(2+) ages in the three samples are 98.2 ± 1.0, 59.3 ± 0.8 Ma and 54.5 ± 0.6 Ma, respectively; 71 zircon grains of Paleogene and Mesozoic age show either positive or negative εHf(t) (from −14.4 to +16.4).

The Weimei quartzarenite (average composition QFL = 87:6:7, QmFLt = 87:6:7) consists of mainly angular to subrounded monocrystalline quartz, with a few feldspars and lithic fragments. Of the 71 concordant ages obtained from sample 13QM03, 70 are pre-Ordovician with a main peak at 537 Ma (Fig. 6). The youngest ages are 229 ± 4 Ma, 450 ± 9 Ma and 493 ± 11 Ma, with discordance of 0%, 0.4% and −0.4%, respectively. The YC1σ(2+) age is 528 ± 5 Ma.

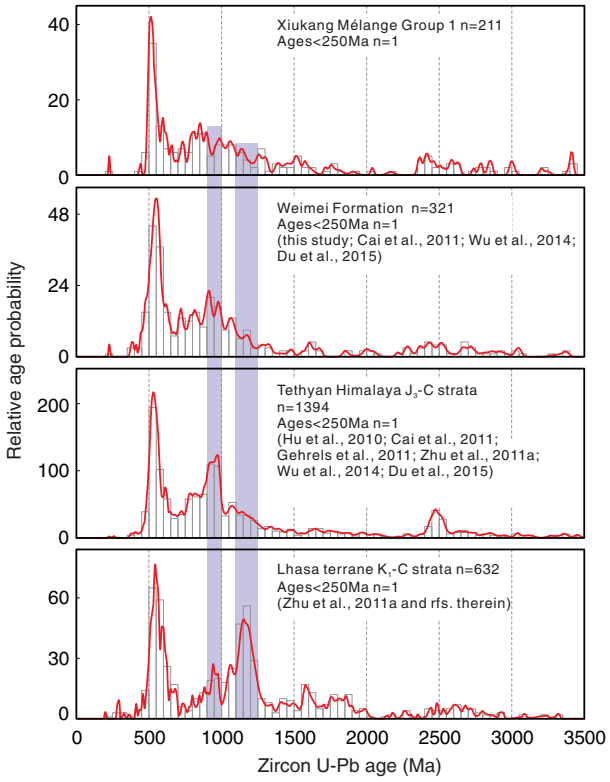

Fig. 6. U–Pb age spectra of detrital zircons in Group 1 quartzarenites. Shown for comparison are data from the Lhasa block (Leier et al., 2007a, b), pre-Cretaceous Tethyan Himalaya successions (Hu et al., 2010; Cai et al., 2011; Gehrels et al., 2011; Zhu et al., 2011a,b; Wu et al., 2014; Du et al., 2015) and Weimei Formation (Cai et al., 2011; Wu et al., 2014; Du et al., 2015; this study). Purple bands outline two age peaks typical of the Lhasa block (1170 Ma) and India (950 Ma) (Zhu et al., 2011b).

5. Discussion

5.1. Provenance of sandstone blocks

In this section, U–Pb age spectra and εHf(t) values of detrital zircons are compared to the patterns shown by all potential sources (including the central and southern Lhasa blocks, the Xigaze forearc basin, the Langjiexue Group, lower Paleogene syncollisional deposits, and Tethyan Himalaya strata) and used as fingerprints to robustly interpret provenance of Group 1, 2, and 3 sandstones. Sandstone petrology provides crucial complementary information to independently constrain our provenance inferences.

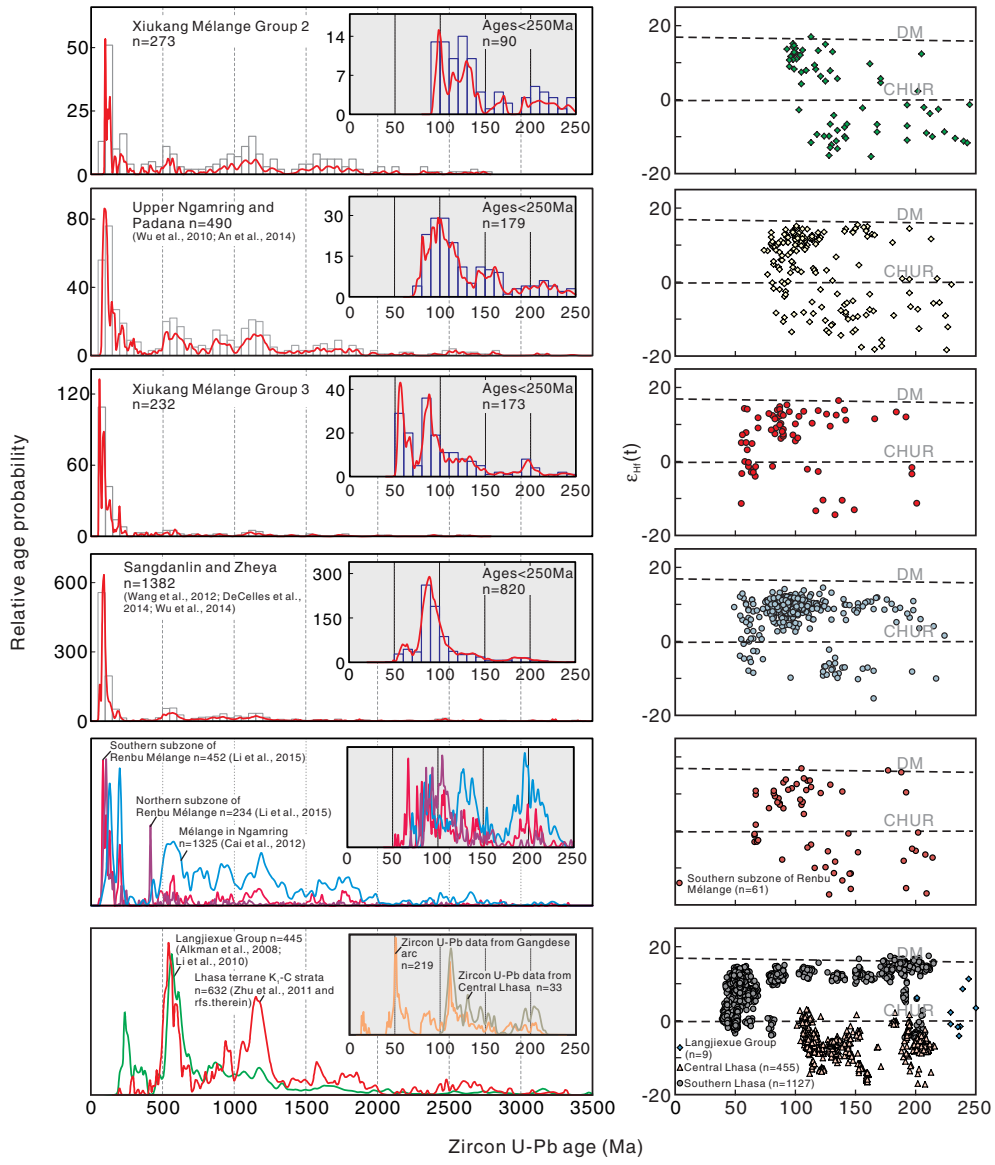

Fig. 7. U–Pb age spectra and Hf isotopic signatures of detrital zircons in Group 2 and Group 3 volcaniclastic sandstones. Data from the Sangdanlin and Zheya Formations (Wang et al., 2011; DeCelles et al., 2014; Wu et al., 2014), Lhasa block (Zhu et al., 2011b and references therein), Gangdese arc (Ji et al., 2009 and references therein), Upper Ngamring and Padana Formations (Wu et al., 2010; An et al., 2014), Langjiexue Group (Aikman et al., 2008; Li et al., 2010), and Xiukang Mélange in Renbu (G.W. Li et al., 2015) and Ngamring (Cai et al., 2012) are shown for comparison.

5.1.1. Zircon signatures of potential source terranes

In the central Lhasa block, Mesozoic magmatic activity took place mostly in the 230–180 Ma and 140–100 Ma time windows, peaking at around 110 Ma (Zhu et al., 2011a and references therein). Most (~75%) zircons in igneous rocks display negative εHf(t) values, with Hf crustal model ages (T_{DM}^{C}) of 2.1–1.4 Ga (Chu et al., 2006; Zhu et al., 2011a). Detrital zircons in the Cretaceous sedimentary succession yield ages between 140 and 105 Ma, with a peak at 120 Ma (Leier et al., 2007a, b). Detrital zircons in Paleozoic strata yield ages in the 500–600 Ma range with a peak at 540 Ma, and in the 1050–1300 Ma range with a peak at 1170 Ma (Zhu et al., 2011a and references therein).

In the southern Lhasa block, magmatic rocks emplaced between the Late Triassic and the Eocene (220–40 Ma) display positive εHf(t) and Hf crustal model ages (T_{DM}^{C}) of 1.0–0.3 Ga (Chu et al., 2006; Zhang et al., 2007; Ji et al., 2009).

Detrital zircons in Cretaceous volcaniclastic turbidites of the Xigaze forearc basin, sourced from the Gangdese arc and the central Lhasa block, display diverse patterns (Wu et al., 2010; Aitchison et al., 2011; An et al., 2014). The lower Ngamring Formation, deposited between 104 and 99 Ma, is characterized by a unimodal age pattern with a 107 Ma peak and positive εHf(t) values. The middle Ngamring Formation, deposited until 88 Ma, is characterized by a bimodal pattern with a subordinate additional peak at 157 Ma and positive εHf(t) values. The upper Ngamring and Padana Formations, deposited until 76 Ma, are characterized by a multimodal pattern with common pre-Mesozoic ages and both positive and negative εHf(t) values.

Detrital zircons from the Langjiexue Group in the Zedang-Renbu area yield ages of 400–200 Ma and positive εHf(t) values (Aikman et al., 2008; Li et al., 2010), whereas those from other parts of the Xiukang Mélange in Renbu (G.W. Li et al., 2015) and Ngamring (Cai et al., 2012) display ages of 230–70 Ma, 700–500 Ma and 1300–800 Ma.

Detrital zircons in Middle Paleocene to Eocene syn-collisional sandstones (e.g. Quxia and Jialazi Formations in the Cuojiangding, Sangdanlin and Zheya Formations in Saga, Enba and Zhaguo Formations in Tingri), sourced from the Gangdese arc and central Lhasa block, include subordinate pre-Mesozoic ages and two groups of Mesozoic

ages. The first group ranges from 201 Ma to 54 Ma with positive εHf(t) values, and the second group from 250 Ma to 92 Ma with negative εHf(t) (Wang et al., 2011; Hu et al., 2012; DeCelles et al., 2014; Wu et al., 2014; Hu et al., 2016, b; J. Li et al., 2015).

Pre-Cretaceous Tethyan Himalayan successions are characterized by the absence of detrital zircons younger than 450 Ma and by three main age groups: 570–480 Ma, clustering around 530 Ma; 1200–750 Ma, clustering around 950 Ma; and 2560–2430 Ma, clustering around 2500 Ma (DeCelles et al., 2000; Aikman et al., 2008; Gehrels et al., 2011; Zhu et al., 2011b). Cretaceous and Lower Paleocene sandstones of the Tethyan Himalaya yield an additional zircon age peak between 140 and 110 Ma (DeCelles et al., 2004; Hu et al., 2010; Clift et al., 2014).

Group 3 feldspatho-litho-quartzose volcaniclastic sandstones yield detrital zircons with dominantly Mesozoic–Paleocene and subordinate pre-Mesozoic ages, and Mesozoic–Cenozoic zircons with both positive and negative εHf(t) values, indicating provenance from the Gangdese magmatic arc and central Lhasa block. The YC1σ(2+) age is ~54 Ma, indicating a post-Paleocene (most likely Early Eocene) depositional age. These features compare well with those of the Quxia and Jialazi Formations in Zhongba, the southern subzone of the Renbu Mélange, and the Sangdanlin and Zheya Formations in Saga, which are in the same tectonic position and interpreted to be part of the Middle Paleocene to Early Eocene syn-collisional basin (Ding et al., 2005; Wang et al., 2011; DeCelles et al., 2014; Wu et al., 2014; G.W. Li et al., 2015; Hu et al., 2015).

5.1.2. Provenance analysis

The petrography of Group 1 quartzarenites is typical of passive-margin deposits fed from a continental block (Dickinson, 1985; Garzanti et al., 2014). Both mineralogical composition and age spectra of detrital zircons compare closely with those of the Weimei Formation in the northern Tethyan Himalaya (Figs. 5, 6 and 8, Cai et al., 2011; Wu et al., 2014; Du et al., 2015). Moreover, the main zircon-age peaks at 514 Ma and 950 Ma are widespread in Tethys Himalayan successions and northern Indian granites and sedimentary units (Cawood et al., 2007). Provenance from the Indian continent is therefore indicated by several consistent lines of evidence. The YC1σ(2+) age of 508 Ma and the absence of zircons in the 140–110 Ma range, typical of Cretaceous/Lower Paleocene Tethyan Himalayan units, constrain the depositional age only very loosely between the Ordovician and the Jurassic.

Because of their detrital modes, detrital-zircon age pattern with a ~99 Ma peak, numerous 190–250 Ma or older ages, and Mesozoic zircons with both positive and negative εHf(t), Group 2 litho-quartzose volcaniclastic sandstones compare well with the upper Ngamring and Padana Formations in the Xigaze forearc-basin (Wu et al., 2010; An et al., 2014), and with sandstone blocks found in the Xiukang Mélange in Ngamring (Cai et al., 2012), and Renbu (G.W. Li et al., 2015). Ultimate provenance from the Zenong Group of the central Lhasa block and Gangdese magmatic arc is indicated. The YC1σ(2+) age of ~94 Ma is quite close to that obtained for the upper Ngamring and Padana Formations of the Xigaze forearc basin, although the slightly different age peaks, more negative εHf(t) values, and numerous pre-Mesozoic detrital zircons suggest greater contribution from the central Lhasa block. In our preferred latest Cretaceous scenario, detritus from the central Lhasa block and Gangdese magmatic arc bypassed the Xigaze forearc basin that had evolved by then to an overfilled terraced stage (An et al., 2014), and was deposited as trench-fill or trench-slope-basin turbidites.

5.2. When did sandstone blocks become part of the Xiukang Mélange?

Pre-Cretaceous turbiditic quartzarenites of Group 1 were originally deposited onto the Indian continental rise and consequently arrived at the southern Asian trench, were off-scraped, thrust and deformed as blocks within the mélange after the onset of the India/Asia collision. Radiolarian chert blocks of Middle–Late Triassic age were also deposited on the Indian continental margin (Zhu et al., 2005), and could not be incorporated into the mélange before collision with Asia. Chert blocks of Late Jurassic–Early Cretaceous age originally deposited on Neotethyan ocean floors, instead, may have reached the trench earlier and thus may have been accreted to the subduction complex or entered the subduction channel prior to collision onset.

Group 2 litho-quartzose volcaniclastic turbidites were derived from the Lhasa block and were originally deposited in the trench and/or on the trench slope during the Late Cretaceous. If deposited in the trench, then Group 2 sandstones together with chert, limestone and basalt blocks may have been episodically off-scraped and accreted into the growing subduction complex before collision (Ziabrev, 2002; Shen et al., 2003a,b; Dupuis et al., 2005, 2006). If deposited on a trench-slope basin, then they could have undergone thrust–fault deformation soon after their deposition. Based on current studies, neither of the two possibilities could be precluded. However, the possibility of original deposition in the trench is here preferred, because trenchfill deposits have been reported adjacent to the mélange in the Ngamring area (Cai et al., 2012).

Group 3 feldspatho-litho-quartzose volcaniclastic sandstones, shed from the Asian margin during the early stages of collision, prograded onto the suture zone and were temporarily deposited in syn-collisional basins but soon involved in deformation, dismembered and incorporated into the mélange as blocks.

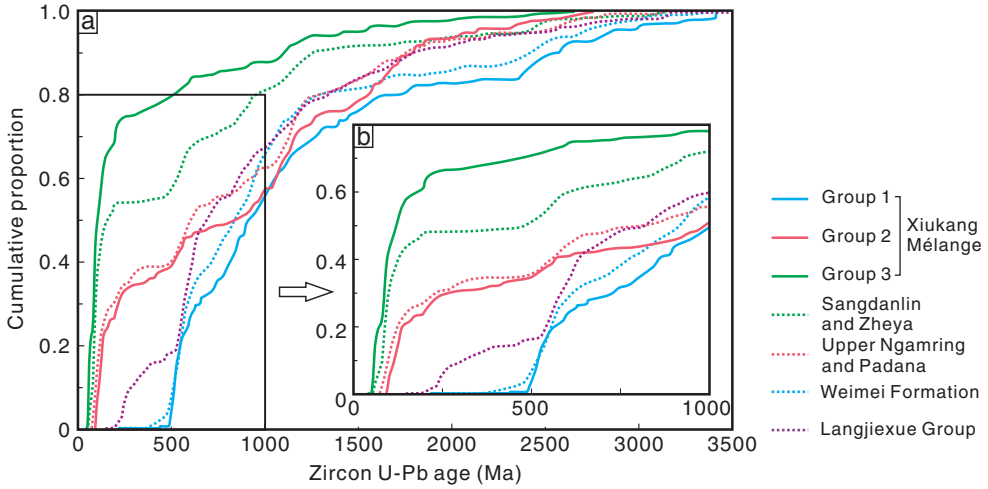

Fig. 8. (a) Cumulative proportions of detrital-zircon ages for sandstone blocks and the same units as in Figs. 6 and 7; (b) The red rectangle in (a) is enlarged in (b).

The Xiukang Mélange was traditionally interpreted as the subduction complex of the Asian margin accreted before the India–Asia collision (Tapponnier et al., 1981; Cai et al., 2012). Our new field observations and provenance analysis, however, indicate that the Xiukang Mélange includes sandstone blocks containing zircons with a YC1σ(2+) age of ~54 Ma, demonstrating that its growth continued into the Early Eocene at least (Fig. 9). Therefore, the Xiukang Mèlange resulted from tectonic processes taking place not only during Neotethyan subduction but also in the early stages of the India/Asia collision. Evidence for growth of the Transhimalayan subduction complex prior to collision is limited to possible accretion of Group 2 sandstones, together with chert, limestone and basalt blocks originally belonging to the Neotethyan oceanic domain.

5.3. Was the active Asian margin accretional or erosional?

The Xiukang Mélange around Colha Pass consists of mostly limestone and sandstone exotic blocks with minor basalt and chert. Blocks containing Middle Permian to Upper Cretaceous limestone overlying OIB-type basalt are interpreted as Neotethyan seamounts accreted – together with chert blocks of Late Jurassic/Early Cretaceous age and Group 2 Gangdese-arc-derived turbidites – to the south Asian margin during subduction (Shen et al., 2003a,b; Dai et al., 2012). During the Late Cretaceous, large volumes of detritus shed by the Lhasa block were trapped in the Xigaze forearc basin, which evolved from the initial sloped stage, to a ridged and terraced stage, and finally to a shelved and benched stage (An et al., 2014). The forearc basin was thus dammed oceanward by a progressively growing subduction complex, which reached close to sea-level prior to collision onset at the end of the Cretaceous. These pieces of evidence indicate that tectonic accretion was taking place at least episodically during Late Cretaceous Neotethyan subduction.

On the other hand, assemblages of oceanic rocks exposed today along the Yarlung-Zangbo suture zone are of limited width (~20 km), indicating that the Upper Cretaceous subduction complex composed of limestone, basalt, chert and occasionally volcaniclastic-sandstone blocks was significantly smaller than modern accretionary prisms undergoing rapid accretion (Schlüter et al., 2002). Subduction erosion occurs along all convergent plate boundaries characterized by high convergence rates and limited sediment supply to the trench (Clift and Vannucchi, 2004; Stern, 2011). If we consider the high subduction rate of Neotethyan lithosphere (Van der Voo et al., 1999) and the relatively small size of the Transhimalayan subduction complex, then we can conclude that the Asian margin in the studied area was with all likelihood largely erosional during much of the Cretaceous, and comparable to modern examples well documented offshore the central Andean cordillera (von Huene and Lallemand, 1990; Ranero and von Huene, 2000). We thus imagine that abyssal and trench sediments, together with seamounts lying on Neotethyan crust, were mainly dragged along the subduction channel and finally underplated at depth or digested in the mantle. Part of this material, however, was episodically off-scraped and accreted into the subduction complex as blocks of Group 2 volcaniclastic sandstone, chert, limestone and basalt (Ziabrev, 2002; Shen et al., 2003a,b; Dupuis et al., 2005, 2006).

6. Conclusion

Field evidence and provenance analysis of sandstone blocks contained in the Xiukang Mélange of the Yarlung-Zangbo suture zone led us to draw the following inferences:

1. Sandstone blocks in the Xiukang Mélange can be divided into three main groups, based on their petrology, detrital-zircon-age pattern and Hf isotope ratios. Group 1 turbiditic quartzarenites were derived from the Indian continent. Instead, Group 2 litho-quartzose volcaniclastic turbidites and Group 3 feldspatho-litho-quartzose volcaniclastic sandstones were both sourced from the Gangdese magmatic arc and the central Lhasa block of the Asian margin, but during distinct stages of its geological evolution.
2. Group 1 turbiditic quartzarenites were deposited in pre-Cretaceous time on the continental rise of the Indian passive margin. Group 2

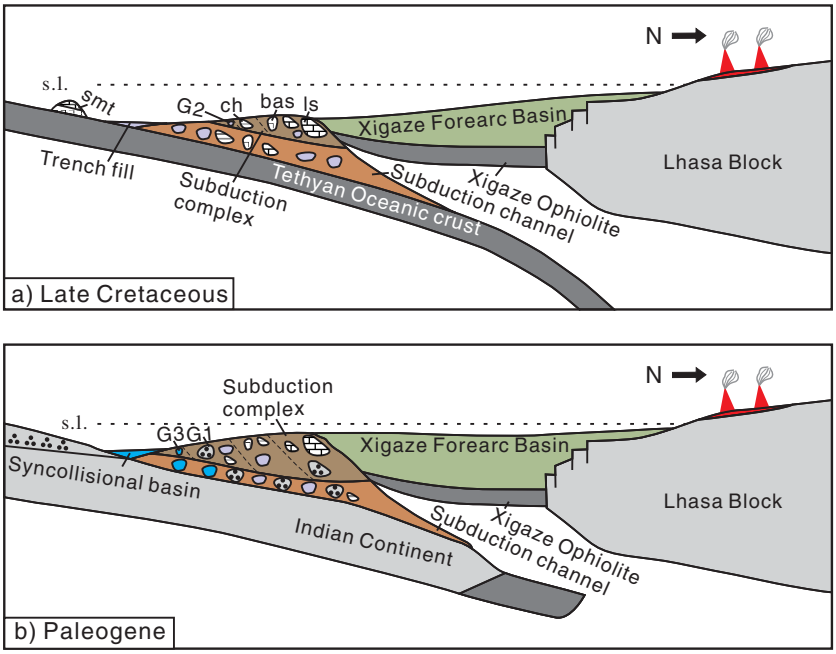

Fig. 9. Schematic reconstruction of the two stages of formation of the Xiukang Mélange, before (a) and after (b) India/Asia collision onset. (a) Before collision, volcaniclastic sandstones fed from the Lhasa Block are mostly trapped in the Xigaze forearc basin but also partly deposited as trench-fill and/or slope-basin turbidites; oceanic sediments are largely swallowed in the subduction channel but also episodically accreted to the subduction complex; (b). During collision onset, quartzarenite turbidites of the Indian continental rise reach the trench and are off-scraped; next, volcaniclastic sandstones derived from the Lhasa block are deposited in the syn-collisional basin and finally incorporated tectonically into the mélange. G1—Group 1 quartzarenite blocks; G2—Group 2 volcaniclastic-sandstone blocks; G3—Group 3 volcaniclastic-sandstone blocks; ch—chert blocks; bas—basalt blocks; lm—limestone blocks; smt—seamount; s.l.—sea level.

Gangdese-arc-derived turbidites were deposited during the Late Cretaceous in the trench and/or on the trench slope of the Transhimalayan active margin well before India/Asia collision onset. Group 3 Gangdese-arc-derived sandstones were deposited not earlier than ~54 Ma, and thus after collision onset. Group 1 and Group 3 sandstones were incorporated into the Xiukang Mélange during the initial stages of the Himalayan Orogeny, whereas Group 2 sandstones may have been accreted at least in part during Neotethyan subduction in the Late Cretaceous.

3. Contrary to what was previously believed, the Xiukang Mélange is the product of both accretion during Cretaceous Neotethyan subduction and deformation during or after the Late Paleocene/Early Eocene early stages of the India/Asia collision. The TransHimalayan margin was largely erosional during the Cretaceous and comparable to the modern active margin of central South America. Abyssal and trench sediments together with seamounts lying on Neotethyan crust, however, were episodically off-scraped to feed a growing subduction complex of sufficient size to trap most detritus shed by the Gangdese arc and Lhasa block in the Xigaze forearc basin.

Acknowledgments

This work benefited from the careful critical reading by two anonymous reviewers and discussions with Jiangang Wang and Xianghui Li. We thank Zhicheng Huang, Bin Wu, Xiong Yan for their assistance in the lab, and Gaoyuan Sun, Juan Li, Zhong Han and Dehua Zhang for their help in the field. This study was financially supported by the NSFC Project (41172092), the CAS Strategic Priority Research Program (B) (XDB03010100) and the MOST 973 Project (2012CB822001).

Appendix A. Supplementary data

Supplementary data to this article can be found online at http://dx.doi.org/10.1016/j.gr.2015.08.010.

References

Aikman, A.B., Harrison, T.M., Lin, D., 2008. Evidence for Early (>44 Ma) Himalayan crustal thickening, Tethyan Himalaya, southeastern Tibet. Earth and Planetary Science Letters 274, 14–23.

Aitchison, J.C., Ali, J.R., Davis, A.M., 2007. When and where did India and Asia collide? Journal of Geophysical Research - Solid Earth 112, B05423. http://dx.doi.org/10.1029/2006JB004706.

Aitchison, J.C., Badengzhu, Davis, A.M., Liu, J.B., Luo, H., Malpas, J.G., McDermid, I.R.C., Wu, H.Y., Ziabrev, S.V., Zhou, M.F., 2000. Remnants of a Cretaceous intra-oceanic subduction system within the Yarlung-Zangbo suture (southern Tibet). Earth and Planetary Science Letters 183, 231–244.

Aitchison, J.C., Xia, X.P., Baxter, A.T., Ali, J.R., 2011. Detrital zircon U–Pb ages along the Yarlung-Tsangpo suture zone, Tibet: implications for oblique convergence and collision between India and Asia. Gondwana Research 20, 691–709.

Amato, J.M., Pavlis, T.L., Clift, P.D., Kochelek, E.J., Hecker, J.P., Worthman, C.M., Day, E.M., 2013. Architecture of the Chugach accretionary complex as revealed by detrital zircon ages and lithologic variations: evidence for Mesozoic subduction erosion in south-central Alaska. Geological Society of America Bulletin 125, 1891–1911.

An, W., Hu, X., Garzanti, E., BouDagher-Fadel, M.K., Wang, J., Sun, G., 2014. Xigaze forearc basin revisited (South Tibet): provenance changes and origin of the Xigaze ophiolite. Geological Society of America Bulletin 126, 1595–1613.

Bédard, É., Hébert, R., Guilmette, C., Lesage, G., Wang, C.S., Dostal, J., 2009. Petrology and geochemistry of the Saga and Sangsang ophiolitic massifs, Yarlung Zangbo Suture Zone, Southern Tibet: evidence for an arc–back-arc origin. Lithos 113, 48–67.

Black, L., Gulson, B., 1978. The age of the mud tank carbonatite, strangways range, northern territory. BMR Journal of Australian Geology and Geophysics 3, 227–232.

Cai, F.L., Ding, L., Leary, R.J., Wang, H., Xu, Q., Zhang, L., Yue, Y., 2012. Tectonostratigraphy and provenance of an accretionary complex within the Yarlung-Zangpo suture zone, southern Tibet: Insights into subduction–accretion processes in the Neo-Tethys. Tectonophysics 574–575, 181–192.

Cai, F.L., Ding, L., Yue, Y., 2011. Provenance analysis of upper Cretaceous strata in the Tethys Himalaya, southern Tibet: implications for timing of India–Asia collision. Earth and Planetary Science Letters 305, 195–206.

Cawood, P.A., Johnson, M.R.W., Nemchin, A.A., 2007. Early Palaeozoic orogenesis along the Indian margin of Gondwana: Tectonic response to Gondwana assembly. Earth and Planetary Science Letters 255, 70–84.

Chu, M.-F., Chung, S.-L., Song, B., Liu, D., O'Reilly, S.Y., Pearson, N.J., Ji, J., Wen, D.-J., 2006. Zircon U–Pb and Hf isotope constraints on the Mesozoic tectonics and crustal evolution of southern Tibet. Geology 34, 745–748.

Clift, P., Vannucchi, P., 2004. Controls on tectonic accretion versus erosion in subduction zones: implications for the origin and recycling of the continental crust. Reviews of Geophysics 42, RG2001. http://dx.doi.org/10.1029/2003RG000127.

Clift, P.D., Carter, A., Jonell, T.N., 2014. U–Pb dating of detrital zircon grains in the Paleocene Stumpata Formation, Tethyan Himalaya, Zanskar, India. Journal of Asian Earth Sciences 82, 80–89.

Clift, P.D., Carter, A., Nicholson, U., Masago, H., 2013. Zircon and apatite thermochronology of the Nankai Trough accretionary prism and trench, Japan: sediment transport in an active and collisional margin setting. Tectonics 32, 377–395.

Dürr, S.B., 1996. Provenance of Xigaze fore-arc basin clastic rocks (Cretaceous, south Tibet). Geological Society of America Bulletin 108, 669–684.

Dai, J.G., Wang, C.S., Li, Y.L., 2012. Relicts of the Early Cretaceous seamounts in the central-western Yarlung Zangbo Suture Zone, southern Tibet. Journal of Asian Earth Sciences 53, 25–37.

Dai, J.G., Wang, C.S., Polat, A., Santosh, M., Li, Y.L., Ge, Y.K., 2013. Rapid forearc spreading between 130–120 Ma: evidence from geochronology and geochemistry of the Xigaze ophiolite, southern Tibet. Lithos 172–173, 1–16.

DeCelles, P.G., Gehrels, G., Quade, J., LaReau, B., Spurlin, M., 2000. Tectonic implications of U–Pb Zircon Ages of the Himalayan Orogenic Belt in Nepal. Science 288, 497–499.

DeCelles, P.G., Gehrels, G.E., Najman, Y., Martin, A.J., Carter, A., Garzanti, E., 2004. Detrital geochronology and geochemistry of Cretaceous–Early Miocene strata of Nepal: implications for timing and diachroneity of initial Himalayan orogenesis. Earth and Planetary Science Letters 227, 313–330.

DeCelles, P.G., Kapp, P., Gehrels, G.E., Ding, L., 2014. Paleocene–Eocene foreland basin evolution in the Himalaya of southern Tibet and Nepal: implications for the age of initial India–Asia collision. Tectonics 33, 824–849.

Dickinson, W.R., 1985. Interpreting provenance relations from detrital modes of sandstones. In: Zuffa, G.G. (Ed.), Provenance of Arenites. Nato ASI, Dordrecht, Reidel, pp. 333–361.

Dickinson, W.R., Gehrels, G.E., 2009. Use of U–Pb ages of detrital zircons to infer maximum depositional ages of strata: a test against a Colorado Plateau Mesozoic database. Earth and Planetary Science Letters 288, 115–125.

Ding, L., Kapp, P., Wan, X., 2005. Paleocene–Eocene record of ophiolite obduction and initial India–Asia collision, south central Tibet. Tectonics 24, TC3001. http://dx.doi.org/10.1029/2004TC001729.

Du, X.J., Chen, X., Wang, C.S., Wei, Y.S., Li, Y.L., Jansa, L., 2015. Geochemistry and detrital zircon U–Pb dating of Lower Cretaceous volcaniclastics in the Babazhadong section, Northern Tethyan Himalaya: implications for the breakup of Eastern Gondwana. Cretaceous Research 52, 127–137.

Dupuis, C., Hébert, R., Dubois-Côté, V., Guilmette, C., Wang, C.S., Li, Z.J., 2006. Geochemistry of sedimentary rocks from mélange and flysch units south of the Yarlung Zangbo suture zone, southern Tibet. Journal of Asian Earth Sciences 26, 489–508.

Dupuis, C., Hebert, R., Duboiscote, V., Wang, C., Li, Y., Li, Z., 2005. Petrology and geochemistry of mafic rocks from mélange and flysch units adjacent to the Yarlung Zangbo Suture Zone, southern Tibet. Chemical Geology 214, 287–308.

Einsele, G., Liu, B., Dürr, S., Frisch, W., Liu, G., Luterbacher, H., Ratschbacher, L., Ricken, W., Wendt, J., Wetzel, A., 1994. The Xigaze forearc basin: evolution and facies architecture (Cretaceous, Tibet). Sedimentary Geology 90, 1–32.

Göpel, C., Allègre, C.J., Xu, R.-H., 1984. Lead isotopic study of the Xigaze ophiolite (Tibet): the problem of the relationship between magmatites (gabbros, dolerites, lavas) and tectonites (harzburgites). Earth and Planetary Science Letters 69, 301–310.

Gao, Y.L., Tang, Y.Q., 1984. Melanges in the southern Xizang (Tibet). In: Guangcen, L., Mercier, J.L. (Eds.), Himalaya Geology II. Geological Publishing House, Beijing, China, pp. 27–44.

Garzanti, E., 2008. Comment on "when and where did India and Asia collide?" by Jonathan C. Aitchison, Jason R. Ali, and Aileen M. Davis. Journal of Geophysical Research 113, B04411. http://dx.doi.org/10.1029/2007JB005276.

Garzanti, E., Baud, A., Mascle, G., 1987. Sedimentary record of the northward flight of India and its collision with Eurasia (Ladakh Himalaya, India). Geodinamica Acta 1, 297–312.

Garzanti, E., Vermeesch, P., Padoan, M., Resentini, A., Vezzoli, G., Ando, S., 2014. Provenance of Passive-Margin Sand (Southern Africa). Journal of Geology 122, 17–42.

Gehrels, G., Kapp, P., DeCelles, P., Pullen, A., Blakey, R., Weislogel, A., Ding, L., Guynn, J., Martin, A., McQuarrie, N., Yin, A., 2011. Detrital zircon geochronology of pre-Tertiary strata in the Tibetan–Himalayan orogen. Tectonics 30, TC5016. http://dx.doi.org/10.1029/2011TC002868.

Girardeau, J., Mercier, J., Yougong, Z., 1985a. Origin of the Xigaze ophiolite, Yarlung Zangbo suture zone, southern Tibet. Tectonophysics 119, 407–433.

Girardeau, J., Mercier, J., Yougong, Z., 1985b. Structure of the Xigaze ophiolite, Yarlung Zangbo suture zone, southern Tibet, China: genetic implications. Tectonics 4, 267–288.

Griffin, W., Pearson, N., Belousova, E.A., Saeed, A., 2007. Reply to "comment to short-communication 'comment: Hf-isotope heterogeneity in zircon 91500' by W.L., Griffin, N.J. Pearson, E.A. Belousova and A. Saeed (Chemical geology 233, 358–363)" by F. Corfu. Chemical Geology 244, 354–356.

Guo, T.Y., Liang, D.Y., Zhang, Y.Z., Zhao, C.H., 1991. Geology of Nagri, Tibet (Xizang). China University of Geosciences Press, Wuhan, China, p. 64.

Hébert, R., Bezard, R., Guilmette, C., Dostal, J., Wang, C., Liu, Z., 2012. The Indus–Yarlung Zangbo ophiolites from Nanga Parbat to Namche Barwa syntaxes, southern Tibet: first synthesis of petrology, geochemistry, and geochronology with incidences on geodynamic reconstructions of Neo-Tethys. Gondwana Research 22, 377–397.

Hu, X., Jansa, L., Chen, L., Griffin, W.L., O'Reilly, S.Y., Wang, J., 2010. Provenance of Lower Cretaceous Wölong volcaniclastics in the Tibetan Tethyan Himalaya: implications for the final breakup of Eastern Gondwana. Sedimentary Geology 223, 193–205.

Hu, X., Jansa, L., Wang, C., 2008. Upper Jurassic–Lower Cretaceous stratigraphy in southeastern Tibet: a comparison with the western Himalayas. Cretaceous Research 29, 301–315.
Hu, X., Sinclair, H.D., Wang, J., Jiang, H., Wu, F., 2012. Late Cretaceous–Palaeogene stratigraphic and basin evolution in the Zhepure Mountain of southern Tibet: implications for the timing of India–Asia initial collision. Basin Research 24, 520–543.
Hu, X., Wang, J., BouDagher-Fadel, M.K., Garzanti, E., An, W., 2016. New insights into the timing of the India–Asia collision from the Paleogene Quxia and Jialazi formations of the Xigaze forearc basin, South Tibet. Gondwana Research 32, 76–92.
Hu, X., Garzanti, E., Moore, T., Raffi, I., 2015. Direct stratigraphic dating of India–Asia collision onset at the Selandian (middle Paleocene; 59 ± 1 Ma). Geology 43, 859–862.
Huang, B., Chen, J., Yi, Z., 2010. Paleomagnetic discussion of when and where India and Asia initially collided. Chinese Journal Geophysics 53, 2045–2058.
Ingersoll, R.V., Fullard, T.F., Ford, R.L., Grimm, J.P., Pickle, J.D., Sares, S.W., 1984. The effect of grain size on detrital modes; a test of the Gazzi-Dickinson point-counting method. Journal of Sedimentary Petrology 54, 103–116.
Jackson, S.E., Pearson, N.J., Griffin, W.L., Belousova, E.A., 2004. The application of laser ablation-inductively coupled plasma-mass spectrometry to in situ U–Pb zircon geochronology. Chemical Geology 211, 47–69.
Jadoul, F., Berra, F., Garzanti, E., 1998. The Tethys Himalayan passive margin from Late Triassic to Early Cretaceous (South Tibet). Journal of Asian Earth Sciences 16, 173–194.
Ji, W., Wu, F., Chung, S., Li, J., Liu, C., 2009. Zircon U–Pb geochronology and Hf isotopic constraints on petrogenesis of the Gangdese batholith, southern Tibet. Chemical Geology 262, 229–245.
Jin, X.C., Huang, H., Shi, Y.K., Zhan, L., 2015. Origin of Permian exotic limestone blocks in the Yarlung Zangbo Suture Zone, Southern Tibet, China: with biostratigraphic, sedimentary and regional geological constraints. Journal of Asian Earth Sciences 106, 22–38.
Leier, A., DeCelles, P.G., Kapp, P., Gehrels, G., 2007a. Lower Cretaceous strata in the Lhasa Terrane, Tibet, with implications for understanding the early tectonic history of the Tibetan Plateau. Journal of Sedimentary Research 77, 809–825.
Leier, A.L., Kapp, P., Gehrels, G., DeCelles, P.G., 2007b. Detrital zircon geochronology of Phanerozoic sedimentary strata in the Lhasa terrane and implications for the tectonic evolution of southern Tibet. Basin Research 19, 361–378.
Li, G.W., Liu, X., Pullen, A., Wei, L., Liu, X., Huang, F., Zhou, X., 2010. In-situ detrital zircon geochronology and Hf isotopic analyses from Upper Triassic Tethys sequence strata. Earth and Planetary Science Letters 297, 461–470.
Li, G.W., Sandiford, M., Boger, S., Liu, X., Wei, L., 2015a. Provenance of the Upper Cretaceous to Lower Tertiary sedimentary relicts in the Renbu Mélange Zone, within the Indus-Yarlung Suture Zone. The Journal of Geology 123, 39–54.
Li, J., Hu, X.M., Garzanti, E., An, W., Wang, J.G., 2015b. Paleogene carbonate microfacies and sandstone provenance (Gamba area, South Tibet): stratigraphic response to initial India–Asia continental collision. Journal of Asian Earth Science 104, 39–54.
Lippert, P.C., van Hinsbergen, D.J.J., Dupont-Nivet, G., 2014. Early Cretaceous to present latitude of the central proto-Tibetan Plateau: a paleomagnetic synthesis with implications for Cenozoic tectonics, paleogeography, and climate of Asia. Geological Society of America Special Papers 507. http://dx.doi.org/10.1130/2014.2507(01).
Liu, G., Einsele, G., 1994. Sedimentary history of the Tethyan basin in the Tibetan Himalayas. Geologische Rundschau 83, 32–61.
Ludwig, K.R., 2011. Isoplot/Ex Version 4: A Geochronological Toolkit for Microsoft Excel. Geochronology Center, Berkeley.
Malpas, J., Zhou, M.-F., Robinson, P.T., Reynolds, P.H., 2003. Geochemical and geochronological constraints on the origin and emplacement of the Yarlung Zangbo ophiolites, Southern Tibet. Geological Society, London, Special Publications 218, 191–206.
Mo, X., Niu, Y., Dong, G., Zhao, Z., Hou, Z., Zhou, S., Ke, S., 2008. Contribution of syncollisional felsic magmatism to continental crust growth: a case study of the Paleogene Linzizong volcanic succession in southern Tibet. Chemical Geology 250, 49–67.
Najman, Y., Appel, E., Boudagher-Fadel, M., Bown, P., Carter, A., Garzanti, E., Godin, L., Han, J., Liebke, U., Oliver, G., Parrish, R., Vezzoli, G., 2010. Timing of India–Asia collision: geological, biostratigraphic, and palaeomagnetic constraints. Journal of Geophysical Research, Solid Earth 115. http://dx.doi.org/10.1029/2010JB007673.
Najman, Y., Carter, A., Oliver, G., Garzanti, E., 2005. Provenance of Eocene foreland basin sediments, Nepal: constraints to the timing and diachroneity of early Himalayan orogenesis. Geology 33, 309–312.
Nicolas, A., Girardeau, J., Marcoux, J., Dupre, B., Xibin, W., Yougong, C., Haixiang, Z., Xuchang, X., 1981. The Xigaze ophiolite (Tibet): a peculiar oceanic lithosphere. Nature 294, 414–417.
Okada, H., 1989. Anatomy of trench-slope basins: examples from the Nankai Trough. Palaeogeography, Palaeoclimatology, Palaeoecology 71, 3–13.
Orme, D.A., Carrapa, B., Kapp, P., 2014. Sedimentology, provenance and geochronology of the upper Cretaceous–lower Eocene western Xigaze forearc basin, southern Tibet. Basin Research. http://dx.doi.org/10.1111/bre.12080.
Pan, G., Ding, J., Yao, D., Wang, L., 2004. The Guide Book of 1:1,500,000 Geologic Map of the Qinghai–Xizang (Tibet) Plateau and Adjacent Areas. Chengdu Cartographic Publishing House, Chengdu.
Pan, G., Mo, X., Hou, Z., Zhu, D., Wang, L., Li, G., Zhao, Z., Geng, Q., Liao, Z., 2006. Spatial–temporal framework of the Gangdese Orogenic Belt and its evolution. Acta Petrologica Sinica 22, 521–533.
Ranero, C., von Huene, R., 2000. Subduction erosion along the Middle America convergent margin. Nature 404, 748–752.
Ratschbacher, L., Frisch, W., Liu, G., Chen, C., 1994. Distributed deformation in southern and western Tibet during and after the India–Asia collision. Journal of Geophysical Research, Solid Earth 99, 19917–19945.
Schärer, U., Xu, R.-H., Allègre, C.J., 1984. UPb geochronology of Gangdese (Transhimalaya) plutonism in the Lhasa–Xigaze region, Tibet. Earth and Planetary Science Letters 69, 311–320.
Schlüter, H.U., Gaedicke, C., Roeser, H.A., Schreckenberger, B., Meyer, H., Reichert, C., Djajadihardja, Y., Prexl, A., 2002. Tectonic features of the southern Sumatra–western Java forearc of Indonesia. Tectonics 21. http://dx.doi.org/10.1029/2001TC901048.
Searle, M.P., Windley, B.F., Coward, M.P., Cooper, D.J.W., Rex, A.J., Rex, D., Tingdong, L.I., Xuchang, X., Jan, M.Q., Thakur, V.C., Kumar, S., 1987. The closing of Tethys and the tectonics of the Himalaya. Geological Society of America Bulletin 98, 678.
Shen, S., Dongli, S., Shi, G.R., 2003a. A biogeographically mixed late Guadalupian (late Middle Permian) brachiopod fauna from an exotic limestone block at Xiukang in Lhaze county, Tibet. Journal of Asian Earth Sciences 21, 1125–1137.
Shen, S., Shi, G.R., Archbold, N.W., 2003b. A Wuchiapingian (Late Permian) brachiopod fauna from an exotic block in the Indus–Tsangpo suture zone, southern Tibet, and its palaeobiogeographical and tectonic implications. Palaeontology 46, 225–256.
Snow, C.A., Wakabayashi, J., Ernst, W.G., Wooden, J.L., 2010. Detrital zircon evidence for progressive underthrusting in Franciscan metagraywackes, west-central California. Geological Society of America Bulletin 122, 282–291.
Stern, C.R., 2011. Subduction erosion: rates, mechanisms, and its role in arc magmatism and the evolution of the continental crust and mantle. Gondwana Research 20, 284–308.
Tapponnier, P., Mercier, J.L., Proust, F., Andrieux, J., Armijo, R., Bassoullet, J.P., Brunel, M., Burg, J.P., Colchen, M., Dupre, B., Girardeau, J., Marcoux, J., Mascle, G., Matte, P., Nicolas, A., Li, T.D., Xiao, X.C., Chang, C.F., Lin, B.Y., Li, G.C., Wang, N.W., Chen, G.M., Han, T.L., Wang, X.B., Deng, W.M., Zheng, H.X., Sheng, H.B., Cao, Y.G., Zhou, J., Qiu, H.R., 1981. The Tibetan side of the India–Eurasia collision. Nature 294, 405–410.
Underwood, M.B., Moore, G.F., 1995. Trenches and trench-slope basins. In: Busby, C.J., Ingersoll, R.V. (Eds.), Tectonics of Sedimentary Basins. Blackwell Science, Cambridge, pp. 179–220.
Van der Voo, R., Spakman, W., Bijwaard, H., 1999. Tethyan subducted slabs under India. Earth and Planetary Science Letters 171 (1), 7–20.
von Huene, R., Lallemand, S., 1990. Tectonic erosion along the Japan and Peru convergent margins. Geological Society of America Bulletin 102, 704–720.
von Huene, R., Scholl, D.W., 1991. Observations at convergent margins concerning sediment subduction, subduction erosion, and the growth of continental crust. Reviews of Geophysics 29, 279–316.
Wang, C.S., Li, X.H., Hu, X.M., Jansa, L.F., 2002. Latest marine horizon north of Qomolangma (Mt Everest): implications for closure of Tethys seaway and collision tectonics. Terra Nova 14, 114–120.
Wang, C.S., Li, X.H., Liu, Z.F., Li, Y.L., Jansa, L., Dai, J.G., Wei, Y.S., 2012. Revision of the Cretaceous–Paleogene stratigraphic framework, facies architecture and provenance of the Xigaze forearc basin along the Yarlung Zangbo suture zone. Gondwana Research 22, 415–433.
Wang, J.G., Hu, X.M., Jansa, L., Huang, Z.C., 2011. Provenance of the Upper Cretaceous–Eocene deep-water sandstones in Sangdanlin, Southern Tibet: constraints on the timing of initial India–Asia collision. The Journal of Geology 119, 293–309.
Wang, Y.J., Mu, X.N., 1980. Some new observation on the Permian biostratigraphy of the Himalayan province in southern Tibet. Journal of Stratigraphy 4, 145–151.
Wen, D., Liu, D., Chung, S., Chu, M., Ji, J., Zhang, Q., Song, B., Lee, T.-Y., Yeh, M., Lo, C., 2008. Zircon SHRIMP U–Pb ages of the Gangdese Batholith and implications for Neotethyan subduction in southern Tibet. Chemical Geology 252, 191–201.
Willems, H., Zhou, Z., Zhang, B., Gräfe, K.U., 1996. Stratigraphy of the upper cretaceous and lower tertiary strata in the Tethyan Himalayas of Tibet (Tingri area, China). Geologische Rundschau 85, 723–754.
Wu, F.Y., Ji, W.Q., Liu, C.Z., Chung, S.L., 2010. Detrital zircon U–Pb and Hf isotopic data from the Xigaze fore-arc basin: constraints on TransHimalayan magmatic evolution in southern Tibet. Chemical Geology 271, 13–25.
Wu, F.Y., Ji, W.Q., Wang, J.G., Liu, C.Z., Chung, S.L., Clift, P.D., 2014. Zircon U–Pb and Hf isotopic constraints on the onset time of India–Asia collision. American Journal of Science 314, 548–579.
XBGMR, 1979. Regional Geology Report of the People's Republic of China: 1:1,000,000 (Xigaze H-45, Yadong G-45), Beijing, p. 230.
Yang, T., Ma, Y., Zhang, S., Bian, W., Yang, Z., Wu, H., Li, H., Chen, W., Ding, J., 2015. New insights into the India–Asia collision process from Cretaceous paleomagnetic and geochronologic results in the Lhasa terrane. Gondwana Research 28 (2), 625–641.
Yin, A., Harrison, M., 2000. Geologic evolution of the Himalayan-Tibetan orogen. Annual Review of Earth and Planetary Sciences 28, 211–280.
Yin, J., Sun, Y., 1988. The Triassic system of the Zhongbei area, Lhaze county, south Tibet. Journal of Institute Geology Chinese Academy Sciences 3, 73–79.
Zhang, H., Xu, W., Guo, J., Zong, K., Cai, H., Yuan, H., 2007. Zircon U–Pb and Hf isotopic composition of deformed granite in the southern margin of the Gangdese belt, Tibet: evidence for early Jurassic subduction of Neo-Tethyan oceanic slab. Acta Petrologica Sinica 23, 1347–1353.
Zhang, Q., Willems, H., Ding, L., Gräfe, K.U., Appel, E., 2012. Initial India–Asia continental collision and foreland basin evolution in the Tethyan Himalaya of Tibet: evidence from stratigraphy and paleontology. The Journal of Geology 120, 175–189.
Zhu, D.C., Pan, G.T., Chung, S.L., Liao, Z., Wang, L., Li, G., 2008. SHRIMP zircon age and geochemical constraints on the origin of Lower Jurassic volcanic rocks from the Yeba Formation, southern Gangdese, South Tibet. International Geology Review 50, 442–471.
Zhu, D.C., Zhao, Z.D., Niu, Y., Mo, X.X., Chung, S.L., Hou, Z.Q., Wang, L.Q., Wu, F.Y., 2011a. The Lhasa Terrane: record of a microcontinent and its histories of drift and growth. Earth and Planetary Science Letters 301, 241–255.
Zhu, D.C., Zhao, Z.D., Niu, Y., Dilek, Y., Mo, X.X., 2011b. Lhasa terrane in southern Tibet came from Australia. Geology 39, 727–730.
Zhu, D.C., Zhao, Z.D., Niu, Y.L., Dilek, Y., Hou, Z.Q., Mo, X.X., 2013. The origin and pre-Cenozoic evolution of the Tibetan Plateau. Gondwana Research 23, 1429–1454.

Zhu, J., Du, Y.S., Liu, Z.X., Feng, Q.L., Tian, W.X., Li, J. Pl, Wang, C.P., 2005. Mesozoic radiolarian chert from the middle sector of the Yarlung Zangbo suture zone, Tibet and its tectonic implications. Science in China Series D: Earth Sciences 35 (12), 1131–1139.

Ziabrev, S., 2002. Tectonic evolution of Dazhuqu and Bainang terranes, Yarlung Zangbo suture, Tibet as constrained by radiolarian biostratigraphy. Department of Earth Sciences. University of Hong Kong, Hong Kong SAR, China p. 133.

Ziabrev, S.V., Aitchison, J.C., Abrajevitch, A.V., Badengzhu, Davis, Luo, A.M.H., 2004. Bainang Terrane, Yarlung–Tsangpo suture, southern Tibet (Xizang, China): a record of intra-Neotethyan subduction–accretion processes preserved on the roof of the world. Journal of the Geological Society 161, 523–539.